PROCEEDINGS OF THE IV INTERNATIONAL CONFERENCE/HIGH TEMPERATURE CAPILLARITY

JOURNAL OF MATERIALS SCIENCE **40** (2005) 2227–2231

Effects of sulfur on interfacial energy between Fe-C melt and graphite

S. JUNG, T. ISHIKAWA*, S. SEKIZUKA*, H. NAKAE
Department of Materials Sci. and Eng., Waseda Univ., Tokyo, Japan

We used an improved sessile drop method, which can measure the equilibrium contact angle of molten Fe-C-S alloys on graphite basal planes using an equilibrated method. We adopted this method for the measurement of the interfacial energy, $\gamma_{s/l}$, between the basal plane of graphite and the Fe-C melts at 1573 K in a purified He-3%H_2 atmosphere. For the calculation of $\gamma_{s/l}$, we have to use the true graphite surface energy, $\gamma_{s/v}$ and the surface tension of the iron melt, $\gamma_{l/v}$, as the reference. However, we could not get a reliable $\gamma_{s/l}$ value from the literature, because the $\gamma_{s/v}$ value could be changed by the contamination of the vapor from the melt. For this reason, we measured the $\gamma_{s/v}$ value using a nonequilibrated method based on the interfacial energy balance at the trijunction using $\gamma_{l/v}$ and the contact angle θ and ϕ, where θ is the contact angle between the liquid metal and graphite substrate observed during the measurement by an optical microscope, and ϕ is the hidden angle observed at cross section of the sample.

We found that the $\gamma_{s/v}$ and $\gamma_{s/l}$ values decrease when the sulfur contents are greater than 10 mass ppm sulfur. From 10 to 120 ppm sulfur, the decreasing rate has a constant value on a logarithmic scale of sulfur activities. The morphology of the graphite changes from spheroidal to flake as $\gamma_{s/l}$ decreases due to increase in the sulfur content.

1. Introduction

Graphite morphologies such as flake or spheroidal determine its mechanical properties and applications in industry. Therefore, an accurate theoretical understanding is needed for changes in the graphite morphology. Many theories have been proposed about the formation of spheroidal graphite. Among them, those related to the interfacial energy event have confirmed that the interfacial energy between the melt and graphite would determine the graphite morphologies [1–5].

Buttner *et al.* [1], who conducted one of the first studies on the morphological changes in graphite, reported the contact angle between the melt and the graphite varied with the addition of magnesium. This change in wetting characteristics was attributed to an increase in $\gamma_{s/l}$. It was theorized that a critical interfacial energy exists above which spheroidal graphite is stable, and below which flake graphite is stable. Keverian *et al.* [2] reported the influence of sulfur on the surface tension of the Fe-C alloy. Since sulfur has a high solubility in Fe-C alloys and act as a surfactant, a dramatic decrease in surface tension is achieved with an increase in the sulfur concentrations. McSwain *et al.* [3] showed that the basal plane of graphite was a preferred growth plane when its interfacial energy is lower than that of the prism plane. According to van Rooyen *et al.* [4] the interfacial energy between the spheroidal graphite and iron melt, $\gamma_{s/l}$, is higher than that of the flake graphite/iron melt. A theoretical consideration was also done for the critical volume and the thermodynamic stability of graphite. Selcuk [5] reported that the graphite morphological changes are closely related with the changes in the graphite-melt interfacial energies. Increases in the interfacial energies have been explained in terms of the elimination of sulfur in the Fe-C melt. However, the interfacial energy of the Mg or Ce treated alloy is gradually reduced with time due to evaporation and oxidation.

Based on the reports mentioned above, the interfacial energy between the liquid iron and the graphite has been studied by the sessile drop method because of the interest in the nucleation and growth of spheroidal graphite in the melt. Typically, spheroidal graphite was reported to form a thermodynamic stable morphology when a higher interfacial energy between the liquid iron and the graphite occurred by elimination of the surfactant, such as sulfur and oxygen.

Until now, the resultant change in the $\gamma_{s/l}$ value could be calculated using the corresponding change in $\gamma_{l/v}$ [2–5], $\gamma_{s/v}$ [6] and the contact angle measured between the melt and the graphite, if $\gamma_{s/v}$ is constant despite a change in the liquid composition. However, the assumption that the $\gamma_{s/v}$ remains constant when the liquid composition changes, would be an oversimplification and may lead to erroneous $\gamma_{s/l}$ values. The surface energy of graphite could be immediately altered by the

**Present address*: IBM Business Consulting Service KK, Tokyo, Japan.

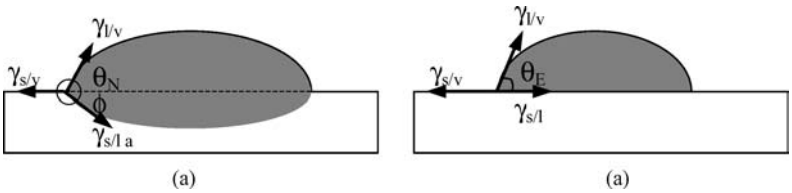

Figure 1 Schematic drawing of the equilibrium shape of a liquid sessile drop: (a) Non-equilibrated sessile drop method and (b) Equilibrated sessile drop method.

adsorption of the melt vapor by the chemical transport via the gas phase, especially for high vapor pressure elements such as magnesium and sulfur, or by surface diffusion. Furthermore, there are problems for measuring the interfacial energy because most experiments using the sessile drop method have been conducted by placing the solid metal on the graphite plate and then heating up to melting. This method may cause an effect when measuring the true contact angle due to mass transfer and chemical reaction between the metal and graphite before the measurement of the contact angle.

For this reason the true $\gamma_{s/l}$ value for a given content of the Fe-C alloy in sulfur is obtained using the $\gamma_{s/v}$ value, which corresponds to the same S content. This will be accomplished by using an improved sessile drop method [7], in which the alloy is melted in an Al_2O_3 tube and then dropped on a graphite plate forming advancing contact angle.

The Neumann triangle relation [8, 9] and Young's equation [10] shown in Fig. 1 was used for the calculation of the interfacial energy, $\gamma_{s/l}$. If the liquid is not saturated, the solid will be dissolved into the liquid, then the equilibrium shape involves a finite curvature for the solid-liquid interface (Fig. 1a). The Neumann relation could be used for the calculation of interfacial energy, $\gamma_{s/v}$, in nonequilibrated sessile drop method. If the liquid is saturated in equilibrated sessile drop method, there is no dissolution and the interface remains flat. In this case, the Young's equation allows calculating interfacial energy, $\gamma_{s/l}$ (Fig. 1b). θ_E is the contact angle between the melts and graphite in the equilibrated system, and θ_N is the contact angle between the melts and graphite in the nonequilibrated system. These contact angles are observed during the measurement by an optical microscope and ϕ is the hidden angle observed at cross section of the sample. First, using the nonequilibrated sessile drop method, we can calculate $\gamma_{s/v}$ from $\gamma_{l/v}$, the measured θ_N and ϕ, while we cannot calculate $\gamma_{s/la}$ because $\gamma_{s/la}$ is the interfacial energy between the melt and a high index plane of the graphite produced by dissolution. Using the equilibrated sessile drop method, we can then calculate $\gamma_{s/l}$ from $\gamma_{s/v}$, θ_E, and $\gamma_{l/v}$. The results gained in the present study would provide further data on the interfacial energy and contact angle between the sulfur containing Fe-C alloys and the basal plane of graphite.

2. Experimental procedures

2.1. Materials for contact angle measurement

The 120 mass ppm sulfur bearing Fe-C alloy and electrolytic iron were used as parent materials and the chemical compositions are shown in Table I. The samples were melted through different ratio of the two irons and cast into graphite molds that were 5 mm in diameter and 300 mm in length using a 3 kg high frequency vacuum induction furnace. The chemical compositions of the samples used for present study are shown in Table II. Pyrolytic graphite plates, with dimensions of $20 \times 20 \times 5$ mm and parallel to the basal plane, were used for the substrate. The plates were ground and polished with 1 μm diamond paste. The samples and the graphites were cleaned in acetone within an ultrasonic cleaner before the experiment.

2.2. Experimental procedure

A schematic of the improved sessile drop method is shown in Fig. 2 and the apparatus and experimental techniques were identical with our previous report [7]. The system consists of a sealed chamber, a gas purification system for the atmospheric gas (He-3%H_2), a set of vacuum pumps to evacuate the chamber, and a 35 mm camera with bellows and macro lenses. The chamber has four windows and contains a dropping device and a molybdenum cylindrical heater with five concentric reflectors located around the dropping device. A thermocouple was located adjacent to the graphite plate holder to monitor the temperature of the specimen throughout each experiment.

The dropping device consists of a pure Al_2O_3 (99.9 mass%) tube with a 0.5 mm hole at its base. When the temperature of the graphite plate reached the experimental temperature, the sample weighing 0.2 ± 0.005 g placed inside of the upper part of the dropping device was pushed along the tube by a steel rod using a magnet and dropped into the bottom of the tube with a graphite lump.

TABLE I Chemical compositions of parent materials, mass%

	Element				
Material	C	Si	Mn	P	S
Electrolytic iron	0.001	0.0002	0.0001	0.0001	0.0001
Fe-C-S iron	4.45	0.016	0.01	0.01	0.012

TABLE II Chemical compositions of experimental irons, mass%

	Samples			
Element	1 ppm S	25 ppm S	50 ppm S	120 ppm S
C	0.001	0.95	2.03	4.45
S	0.0001	0.0026	0.0050	0.012

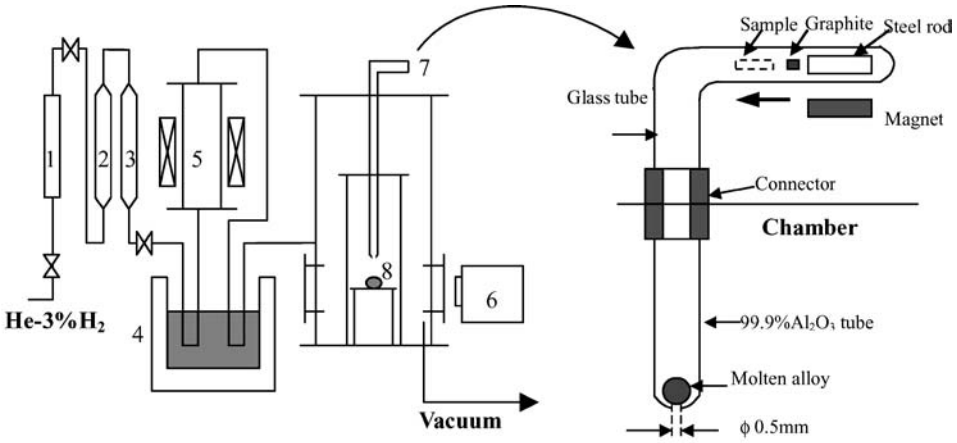

Figure 2 Improved sessile drop method apparatus.

The gas purification system consists of a molecular sieve for trapping H_2O and O_2, a liquid nitrogen cold trap and a titanium furnace heated to about 1173 K to remove O_2 from the atmospheric gas. Another liquid nitrogen cold trap was placed before the chamber to eliminate H_2O vapor from the Ti furnace and then the purified gas was introduced into the chamber.

For the experiment, the pyrolytic graphite plate was set in a horizontal position under the dropping device. The chamber was evacuated to about 1.3×10^{-3} Pa and heated to 1523 K. In the case of the equilibrated experiment, when the temperature of the substrate reached 1573 K, the sample was introduced into the bottom of the Al_2O_3 tube and saturated with the graphite lumps for 30 min for the equilibrated system. He-3%H_2 gas was then introduced into the chamber up to 1.05 atm and the carbon saturated melt was slowly forced out through the hole of the Al_2O_3 tube by a gradual decrease in the atmospheric pressure of the chamber. Therefore, only advancing contact angles can be measured by this technique without contaminating the graphite surface before the measurement.

The nonequilibrated method was conducted when the temperature was raised to 1523 K and held for 30 min to the saturation. The measurement of contact angle was then conducted by dropping the melt on the graphite substrate at 1523 K and then the temperature was raised to approximately 1573 K at the rate of 1 K/min and held for 30 min. After the measurement, the electric power of the furnace was turned off for cooling.

The contact angles θ_E and θ_N were measured using the projected photos of the 35 mm camera. The hidden angle ϕ of the nonequilibrated system was measured using the center cut cross section. The $\gamma_{l/v}$ values [2] are used for the calculation of the interfacial energy $\gamma_{s/v}$ and $\gamma_{s/l}$.

3. Results

After the nonequilibrated sessile drop experiments, the samples were cut and polished to measure ϕ, the average value of ϕ_1 and ϕ_2, and one of these results is shown in Fig. 3. The shape of the original trijunction, dotted line, cannot be observed, which means the sample contracted during cooling. The contracted distance l, $\Delta C_1 + \Delta C_2$, and the calculated distance by contraction during and after the solidification are shown in Table III. We calculated the distance using the thermal expansion coefficient [11, 12] assuming that the contraction occurs from 1423 K. Both values agree well, if the contraction after the solidification is considered. Table IV shows that the θ_N and ϕ varies with sulfur, which could be attributed to the evolution of the interface mor-

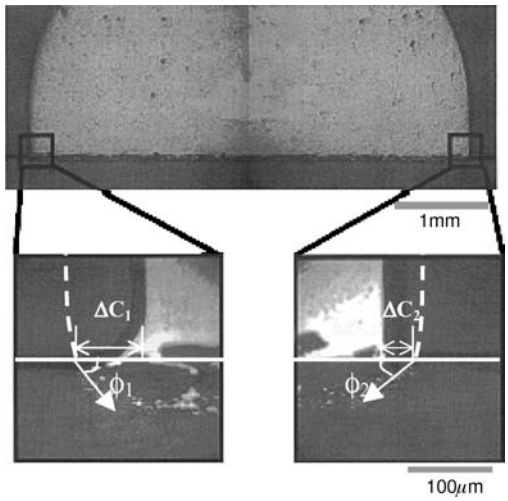

Figure 3 Interfacial morphology of the 1 ppm S sample after nonequilibrated experiment.

TABLE III Change in length of contraction during solidification

	Length		
Samples	Diameter, mm	Contraction, μm (Measured)	Contraction, μm (Calculated)
1 ppm S	4.3	124	107
25 ppm S	4.1	130	102
50 ppm S	4.2	94	104
120 ppm S	4.3	116	107

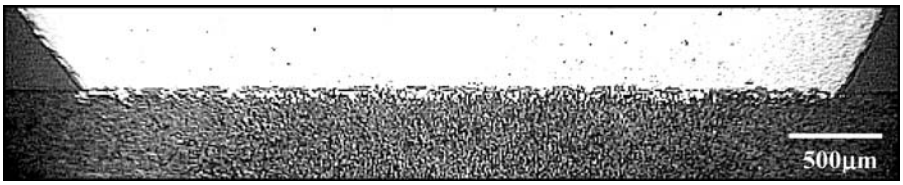

Figure 4 Interfacial morphology of the 1 ppm S sample after equilibrated experiment.

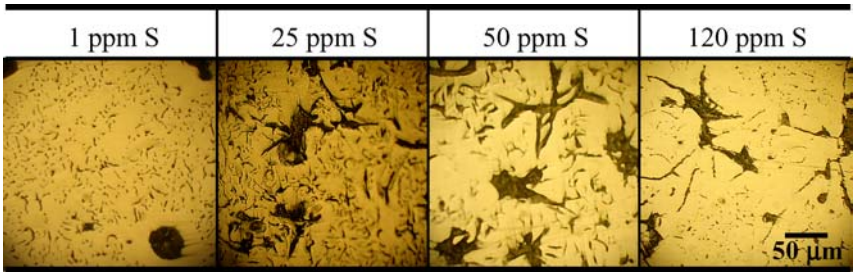

Figure 5 Influence of S content on graphite morphology of the Fe-C alloy.

phology at the trijunction. If the shape of the trijunction is not altered by the contraction, the $\gamma_{s/v}$ values can be calculated from the θ_N and ϕ values and the $\gamma_{l/v}$ [2]. Note that the calculated $\gamma_{s/v}$ values decrease from 1.04 N/m to 0.90 N/m with the increase in the sulfur content.

After the equilibrated sessile drop experiments, the samples were cut vertically to examine the interfacial morphology and one of the samples is shown in Fig. 4. When the interface is compared to that of the non-equilibrated experiment (Fig. 3), the S/L interface is flat and smooth. The carbon pick-up into the melt was nearly zero, indicating a good equilibrium status. During the experiment, the θ_E values were measured and are summarized in Table V. The θ_E values decrease with the increasing sulfur content.

Fig. 5 shows influence of sulfur on graphite morphologies. The graphite in the 1 ppm S specimen is consisted of fine and spheroidal particles, while the graphite morphology changes from spheroidal to flake with the increasing sulfur content.

The $\gamma_{s/l}$ values are calculated by Young's equation using the θ_E (Table V), the $\gamma_{l/v}$ and the $\gamma_{s/v}$ (Table IV) and are drawn as a function of the activity of sulfur in Fig. 6. The activity of sulfur, a_s, was calculated by

TABLE IV Summary of the changes in $\gamma_{s/v}$ values calculated from θ_N, ϕ, and $\gamma_{l/v}$ [2]

	Values				
Samples	a_s	θ_N, deg	ϕ,deg	$\gamma_{l/v}$, N/m [2]	$\gamma_{s/v}$, N/m
1 ppm S	4.5×10^{-4}	94	56	1.73	1.04
25 ppm S	1.1×10^{-2}	97	53	1.65	1.03
50 ppm S	2.3×10^{-2}	98	52	1.51	0.96
120 ppm S	5.4×10^{-2}	100	49	1.32	0.90

TABLE V Contact angle θ_E after the equilibrated sessile drop experiment

Samples	1 ppm S	25 ppm S	50 ppm S	120 ppm S
θ_E, deg	146	132	128	126

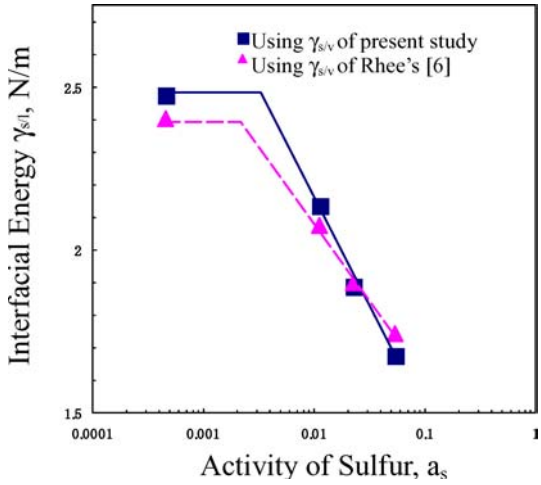

Figure 6 Comparison of $\gamma_{s/l}$ obtained from $\gamma_{s/v}$ value in the present study and Rhee's [6].

the activity coefficient of sulfur, f_s, which is 4.5 in the Fe-4.5%C iron melt [14, 15]. For comparison, the $\gamma_{s/l}$ values are also calculated using the Rhee's $\gamma_{s/v}$ value, 0.934 N/m [6]. The $\gamma_{s/l}$ values calculated using the $\gamma_{s/v}$ values in present study is higher than that of the values using the Rhee's value [6], below a_s of 0.02. Note that a critical interfacial energy exists around 10 ppm sulfur, or a_s of 4.5×10^{-3}, below which flake graphite is stable and above which spheroidal graphite is stable. This critical sulfur content was reported in other researches [16, 17]. More than 10 ppm, the $\gamma_{s/l}$ decreases with increase in sulfur content.

4. Conclusions

The interfacial energy between the basal plane of graphite and the carbon saturated iron melt has been measured using an improved sessile drop method as a function of the sulfur activity. The results obtained herein strengthen the hypothesis that a high graphite-melt interfacial energy favors spheroidal graphite formation.

1. The $\gamma_{s/v}$ values change by the contamination of the iron melt, namely by sulfur contained in the melt . The $\gamma_{s/v}$ values differ from that of Rhee's.

2. The $\gamma_{s/l}$ interfacial energy significantly decrease for sulfur contents higher than 10 ppm, (or for sulfur activities a_s higher than is 4.5×10^{-3})

3. The morphological inspection shows that the graphite morphology changes from spheroidal to flake as the interfacial energy of basal plane decreases.

References

1. F. H. BUTTNER, H. F. TAYLOR and J. WULFF, *Amer. Foundryman* Oct. (1951) 49.
2. J. KEVERIAN and H. F. TAYLOR, *Trans. AFS* **65** (1957) 212.
3. R. H. MCSWAIN and C. E. BATES, in Proceedings of the 2nd International Symposium on the Metallurgy of Cast Iron, (Geneva, 1974) p. 421.
4. G. T. VAN ROOYEN and G. PAUL, *Metal Science* **8** (1974) 370.
5. E. SELCUK, in Proceedings of the 2nd International Symposium on the Metallurgy of Cast Iron, (Geneva, 1974) p. 409.
6. S. K. RHEE, *J. Am. Ceram. Soc.* **55** (1972) 300.
7. H. FUJI, H. NAKAE and K. OKADA, *Acta Mater.* **41** (1993) 2963.
8. L. BORUVKA and A. W. NEUMANN, *J. Chem. Phys.* **66** (1977) 5464.
9. G. LEVI and W. D. KAPLAN, *Acta Mater* **51** (2003) 2793.
10. T. YOUNG, *Phil. Trans. Royal Soc, London* **95** (1805) 65.
11. C. F. WALTON and T. J. OPAR,"Iron Castings Handbook", (Iron Castings Society, 1981)
12. B. E. NEIMARK *et al.*, *Russian Castings Production* (1967) 435.
13. B. J. KEENE, *Int. Mater. Rev.* **33** (1988) 1.
14. J. P. MORRIS and R. C. BUEHL, *Trans. AIME* **188** (1950) 317.
15. S. BANYA and J. CHIPMAN, *Trans. Metall. Soc. AIME* **245** (1969) 133.
16. S. V. SUBRAMANIAN, D. A. R. KAY and G. R. PURDY, *Mat. Res. Soc. Symp. Proc.* **34** (1985) 47.
17. W. OLDFIELD, *Trans. AFS* **79** (1971) 455.

Received 31 March
and accepted 20 October 2004